

Landau Singularities from the Amplituhedron

T. Dennen,¹ I. Prlina, M. Spradlin, S. Stanojevic and A. Volovich

Department of Physics, Brown University, Providence RI 02912, USA

ABSTRACT: We propose a simple geometric algorithm for determining the complete set of branch points of amplitudes in planar $\mathcal{N} = 4$ super-Yang-Mills theory directly from the amplituhedron, without resorting to any particular representation in terms of local Feynman integrals. This represents a step towards translating integrands directly into integrals. In particular, the algorithm provides information about the symbol alphabets of general amplitudes. We illustrate the algorithm applied to the one- and two-loop MHV amplitudes.

¹Current address: Google Inc., Mountain View CA 94043, USA

Contents

1	Introduction	1
1.1	Momentum Twistors	3
1.2	Positivity and the MHV Amplituhedron	4
1.3	Landau Singularities	5
2	Eliminating Spurious Singularities of MHV Amplitudes	7
2.1	The Spurious Pentagon Singularity	8
2.2	The Spurious Three-Mass Box Singularity	10
2.3	A Two-Loop Example	10
2.4	Summary	12
3	An Amplituhedrony Approach	12
3.1	One-Loop MHV Amplitudes	14
3.2	Two-Loop MHV Amplitudes: Configurations of Positive Lines	15
3.3	Two-Loop MHV Amplitudes: Landau Singularities	21
4	Discussion	26
A	Elimination of Bubbles and Triangles	29
A.1	Bubble sub-diagrams	29
A.2	Triangle sub-diagrams	29

1 Introduction

Ever since its conception, the Feynman diagram approach has been the standard paradigm for perturbative calculations in quantum field theory. While the method can, in principle, be used at any order in perturbation theory, the calculations get more and more demanding at each new loop order. Alternately one can seek hidden symmetries and new underlying principles which motivate new calculational approaches where the most basic features of Feynman diagrams, such as unitarity and locality, are emergent instead of manifest. Recent years have seen tremendous success in “reverse engineering” such new symmetries and principles from properties of scattering amplitudes. This approach has been particularly fruitful in simple quantum field theories such as the planar maximally supersymmetric $\mathcal{N} = 4$ super-Yang-Mills (SYM) theory [1].

In particular, it has been realized that the unitarity and locality of the integrands [2] of loop-level amplitudes in SYM theory can be seen to emerge from a very simple geometric principle of positivity [3]. Moreover, it has been proposed that all information about arbitrary integrands in this theory is encapsulated in objects called amplituhedra [4, 5] that have received considerable recent attention; see for example [6–13]. Unfortunately, there remains a huge gap between our understanding of integrands and our understanding of the corresponding integrated amplitudes. Despite great advances in recent years we of course don’t have a magic wand that can be waved at a general integrand to “do the integrals”. Indeed, modern approaches to computing multi-loop amplitudes in SYM theory, such as the amplitude bootstrap [14, 15] even eschew knowledge of the integrand completely. It would be enormously valuable to close this gap between our understanding of integrands and amplitudes.

As a step in that direction, and motivated by [16], we began in [17] to systematically explore how integrands encode the singularities of integrated amplitudes, in particular their branch points. Scattering amplitudes in quantum field theory generally have very complicated discontinuity structure. The discontinuities across branch cuts are given by sums of unitarity cuts [18–23]. These discontinuities may appear on the physical sheet or after analytic continuation to other sheets; these higher discontinuities are captured by multiple unitarity cuts (see for example [24, 25]). A long-standing goal of the S-matrix program, in both its original and modern incarnations, has been to construct expressions for the scattering amplitudes of a quantum field theory based solely only on a few physical principles and a thorough knowledge of their analytic structure.

In [17] we studied the branch cut structure of one- and two-loop MHV amplitudes in SYM theory starting from certain representations of their integrands in terms of local Feynman integrals [26]. We recovered all of their known branch points, but we also encountered many other, spurious branch points that are artifacts of the particular representations used. Indeed, the analysis of [17] was completely insensitive to numerator factors in the integrand, but the numerators are really where all of the action is—in any standard quantum field theory the denominator of a loop integrand is a product of local propagators; the numerator is where all of the magic lies.

Our goal in this paper is to improve greatly on the analysis of [17]. We do this by presenting a method for asking the amplituhedron to directly provide a list of the physical branch points of a given amplitude. In the remainder of section 1 we briefly review the necessary background on momentum twistor notation, the MHV amplituhedron, and Landau singularities. In section 2 we demonstrate how to refine the analysis of [17] by scanning through the list of putative branch points found in that paper, and asking the amplituhedron to identify each one as physical or spurious. This is an

ultimately inefficient approach, but armed with experience from that exercise we turn in section 3 to the development of a general, geometric algorithm for reading off the physical branch points of MHV amplitudes directly from the amplituhedron.

1.1 Momentum Twistors

We begin by reviewing the basics of momentum twistor notation [27], which we use throughout our calculations. Momentum twistors are based on the correspondence between null rays in (complexified, compactified) Minkowski space and points in twistor space (\mathbb{P}^3), or equivalently, between complex lines in \mathbb{P}^3 and points in Minkowski space. We use Z_a, Z_b , etc. to denote points in \mathbb{P}^3 , which may be represented using four-component homogeneous coordinates $Z_a^I = (Z_a^1, Z_a^2, Z_a^3, Z_a^4)$ subject to the identification $Z_a^I \sim tZ_a^I$ for any non-zero complex number t . We use (ab) as shorthand for the bitwistor $\epsilon_{IJKL}Z_a^K Z_b^L$. Geometrically, we can think of (ab) as the (oriented) line containing the points Z_a and Z_b . Similarly we use (abc) as shorthand for $\epsilon_{IJKL}Z_a^J Z_b^K Z_c^L$, which represents the (oriented) plane containing Z_a, Z_b and Z_c . Analogously, $(abc) \cap (def)$ stands for $\epsilon^{IJKL}(abc)_K(def)_L$, which represents the line where the two indicated planes intersect. In planar SYM theory we always focus on color-ordered partial amplitudes so an n -point amplitude is characterized by a set of n momentum twistors $Z_i^I, i \in \{1, \dots, n\}$ with a specified cyclic ordering. Thanks to this implicit cyclic ordering we can use \bar{i} as shorthand for the plane $(i-1 i i+1)$, where indices are always understood to be mod n .

The natural $SL(4, \mathbb{C})$ invariant is the four-bracket denoted by

$$\langle abcd \rangle \equiv \epsilon_{IJKL} Z_a^I Z_b^J Z_c^K Z_d^L. \quad (1.1)$$

We will often be interested in a geometric understanding of the locus where such four-brackets might vanish, which can be pictured in several ways. For example, $\langle abcd \rangle = 0$ only if the two lines (ab) and (cd) intersect, or equivalently if the lines (ac) and (bd) intersect, or if the point a lies in the plane (bcd) , or if the point c lies on the plane (abd) , etc. Computations of four-brackets involving intersections may be simplified via the formula

$$\langle (abc) \cap (def) gh \rangle = \langle abcg \rangle \langle defh \rangle - \langle abch \rangle \langle defg \rangle. \quad (1.2)$$

In case the two planes are specified with one common point, say $f = c$, it is convenient to use the shorthand notation

$$\langle (abc) \cap (dec) gh \rangle \equiv \langle c(ab)(de)(gh) \rangle \quad (1.3)$$

which highlights the fact that this quantity is antisymmetric under exchange of any two of the three lines (ab) , (de) , and (gh) .

1.2 Positivity and the MHV Amplituhedron

In this paper we focus exclusively on MHV amplitudes. The integrand of an L -loop MHV amplitude is a rational function of the n momentum twistors Z_i specifying the kinematics of the n external particles, as well as of L loop momenta, each of which corresponds to some line $\mathcal{L}^{(\ell)}$ in \mathbb{P}^3 ; $\ell \in \{1, \dots, L\}$. The amplituhedron [4, 5] purports to provide a simple characterization of the integrand when the Z_i^I take values in a particular domain called the positive Grassmannian $G_+(4, n)$. In general $G_+(k, n)$ may be defined as the set of $k \times n$ matrices for which all ordered maximal minors are positive; that is, $\langle a_{i_1} \cdots a_{i_k} \rangle > 0$ whenever $i_1 < \cdots < i_k$.

Each line $\mathcal{L}^{(\ell)}$ may be characterized by specifying a pair of points $\mathcal{L}_1^{(\ell)}, \mathcal{L}_2^{(\ell)}$ that it passes through. We are always interested in $n \geq 4$, so the Z_i generically provide a basis for \mathbb{C}^4 . In the MHV amplituhedron a pair of points specifying each $\mathcal{L}^{(\ell)}$ may be expressed in the Z_i basis via an element of $G_+(2, n)$ called the D -matrix:

$$\mathcal{L}_\alpha^{(\ell)I} = \sum_{i=1}^n D_{\alpha i}^{(\ell)} Z_i^I, \quad \alpha = 1, 2. \quad (1.4)$$

For $n > 4$ the Z_i are generically overcomplete, so the map eq. (1.4) is many-to-one.

The L -loop n -point MHV amplituhedron is a $4L$ -dimensional subspace of the $2L(n-2)$ -dimensional space of L D -matrices. We will not need a precise characterization of that subspace, but only its grossest feature, which is that it is a subspace of the space of L mutually positive points in $G_+(2, n)$. This means that it lives in the subspace for which all ordered maximal minors of the matrices

$$(D^{(\ell)}), \quad \begin{pmatrix} D^{(\ell_1)} \\ D^{(\ell_2)} \end{pmatrix}, \quad \begin{pmatrix} D^{(\ell_1)} \\ D^{(\ell_2)} \\ D^{(\ell_3)} \end{pmatrix}, \quad \text{etc.}$$

are positive.

A key consequence of the positivity of the D -matrices is that, for positive external data $Z_i^I \in G_+(4, n)$, all loop variables $\mathcal{L}^{(\ell)}$ are oriented positively with respect to the external data and to each other: inside the amplituhedron,

$$\langle \mathcal{L}^{(\ell)} i i+1 \rangle > 0 \text{ for all } i \text{ and all } \ell, \text{ and} \quad (1.5)$$

$$\langle \mathcal{L}^{(\ell_1)} \mathcal{L}^{(\ell_2)} \rangle > 0 \text{ for all } \ell_1, \ell_2. \quad (1.6)$$

The boundaries of the amplituhedron coincide with the boundaries of the space of positive D -matrices, and occur for generic Z when one or more of these quantities approach zero.

It is worth noting that the above definition of positivity depends on the arbitrary choice of a special point Z_1 , since for example $\langle \mathcal{L} 1 2 \rangle > 0$ but the cyclically related quantity $\langle \mathcal{L} n 1 \rangle$ is negative. The choice of special point is essentially irrelevant: it just means that some special cases need to be checked. In calculations we can sidestep this subtlety by always choosing to analyze configurations involving points satisfying $1 \leq i < j < k < l \leq n$, which can be done without loss of generality. The geometric properties of figures 2–5 below are insensitive to the choice and always have full cyclic symmetry.

The integrand of an MHV amplitude is a canonical form $d\Omega$ defined by its having logarithmic singularities only on the boundary of the amplituhedron. The numerator of $d\Omega$ conspires to cancel all singularities that would occur outside this region (see [9] for some detailed examples). Our analysis will require no detailed knowledge of this form. Instead, we will appeal to “the amplituhedron” to tell us whether or not any given configuration of lines $\mathcal{L}^{(\ell)}$ overlaps the amplituhedron or its boundaries by checking whether eqs. (1.5) and (1.6) are satisfied (possibly with some $=$ instead of $>$).

1.3 Landau Singularities

The goal of this paper is to understand the singularities of (integrated) amplitudes. For standard Feynman integrals, which are characterized by having only local propagators in the denominator, it is well-known that the locus in kinematic space where a Feynman integral can potentially develop a singularity is determined by solving the Landau equations [20, 28, 29] which we now briefly review.

After Feynman parameterization any L -loop scattering amplitude in D spacetime dimensions may be expressed as a linear combination of integrals of the form

$$\int \prod_{r=1}^L d^D l_r \int_{\alpha_i \geq 0} d^\nu \alpha \delta \left(1 - \sum_{i=1}^{\nu} \alpha_i \right) \frac{\mathcal{N}(l_r^\mu, p_i^\mu, \dots)}{\mathcal{D}^\nu} \quad (1.7)$$

where ν is the number of propagators in the diagram, each of which has an associated Feynman parameter α_i , \mathcal{N} is some numerator factor which may depend on the L loop momenta l_r^μ as well as the external momenta p_i^μ , and finally the denominator involves

$$\mathcal{D} = \sum_{i=1}^{\nu} \alpha_i (q_i^2 - m_i^2), \quad (1.8)$$

where q_i^μ is the momentum flowing along propagator i which carries mass m_i . The integral can be viewed as a multidimensional contour integral in the $LD + \nu$ integration variables (l_r^μ, α_i) , where the α_i contours begin at $\alpha_i = 0$ and the l_r^μ contours are considered closed by adding a point at infinity. Although the correct contour for a

physical scattering process is dictated by an appropriate $i\epsilon$ prescription in the propagators, a complete understanding of the integral, including its analytic continuation off the physical sheet, requires arbitrary contours to be considered.

An integral of the above type can develop singularities when the denominator \mathcal{D} vanishes in such a way that the contour of integration cannot be deformed to avoid the singularity. This can happen in two distinct situations:

(1) The surface $\mathcal{D} = 0$ can pinch the contour simultaneously in all integration variables (l_r^μ, α_i). This is called the “leading Landau singularity”, though it is important to keep in mind that it is only a potential singularity. The integral may have a branch point instead of a singularity, or it may be a completely regular point, depending on the behavior of the numerator factor \mathcal{N} .

(2) The denominator may vanish on the boundary when one or more of the $\alpha_i = 0$ and pinch the contour in the other integration variables. These are called subleading Landau singularities.

The Landau conditions encapsulating both possible situations are

$$\sum_{i \in \text{loop}} \alpha_i q_i^\mu = 0 \text{ for each loop, and} \tag{1.9}$$

$$\alpha_i (q_i^2 - m_i^2) = 0 \text{ for each } i. \tag{1.10}$$

For leading singularities eq. (1.10) is satisfied by $q_i^2 - m_i^2 = 0$ for each i , while subleading singularities have one or more i for which $q_i^2 - m_i^2 \neq 0$ but the corresponding $\alpha_i = 0$. We will always refer to equations of type $q_i^2 - m_i^2$ as “cut conditions” since they correspond to putting some internal propagators on-shell. It is important to emphasize that the Landau equations themselves have no knowledge of the numerator factor \mathcal{N} , which can alter the structure of a singularity or even cancel a singularity entirely.

Sometimes (i.e., for some diagram topologies), the Landau equations (1.9) and (1.10) may admit solutions for arbitrary external kinematics p_i^μ . This usually indicates an infrared divergence in the integral (we will not encounter ultraviolet divergences in SYM theory), which may or may not be visible by integration along the physical contour.

In other cases, solutions to the Landau equations might exist only when the p_i^μ lie on some subspace of the external kinematic space. MHV amplitudes in SYM theory are expected to have only branch point type singularities (after properly normalizing them by dividing out a tree-level Parke-Taylor [30] factor), so for these amplitudes we are particularly interested in solutions which exist only on codimension-one slices of the external kinematic space. Even when the p_i^μ live on a slice where solutions of the Landau equations exist, the solutions generally occur for values of the integration variables α_i and l_r^μ that are off the physical contour (for example, the α_i could be complex). This indicates a branch point of the integral that is not present on the

physical sheet but only becomes apparent after suitable analytic continuation away from the physical contour.

Finally let us note that we have ignored a class of branch points called “second-type singularities” [28, 31, 32] which arise from pinch singularities at infinite loop momentum. As argued in [17], these should be absent in planar SYM theory when one uses a regulator that preserves dual conformal symmetry.

2 Eliminating Spurious Singularities of MHV Amplitudes

In principle one can write explicit formulas for any desired integrand in planar SYM theory by triangulating the interior of the amplituhedron and constructing the canonical form $d\Omega$ with logarithmic singularities on its boundary. However, general triangulations may produce arbitrarily complicated representations for $d\Omega$. In particular, these may have no semblance to standard Feynman integrals with only local propagators in the denominator (see [6] for some explicit examples). It is therefore not immediately clear that the Landau equations have any relevance to the amplituhedron. The connection will become clear in the following section; here we begin by revisiting the analysis of [17] with the amplituhedron as a guide.

In [17] we analyzed the potential Landau singularities of one- and two-loop MHV amplitudes by relying on the crutch of representations of these amplitudes in terms of one- and two-loop chiral pentagon and double-pentagon integrals [26]. The solutions to the various sets of Landau equations for these integral topologies represent *potential* singularities of the amplitudes, but this set of potential singularities is too large for two reasons. First of all, the chiral integrals are dressed with very particular numerator factors to which the Landau equations are completely insensitive. Scalar pentagon and double pentagon integrals certainly have singularities that are eliminated by the numerator factors of their chiral cousins. Second, some actual singularities of individual chiral integrals may be spurious in the full amplitude due to cancellations when all of the contributing chiral integrals are summed.

It is a priori highly non-trivial to see which singularities of individual integrals survive the summation to remain singularities of the full amplitude. However, the amplituhedron hypothesis provides a quick way to detect spurious singularities from simple considerations of positive geometry. In this section we refine our analysis of [17] to determine which *potential* singularities identified in that paper are *actual* singularities by appealing to the amplituhedron as an oracle to tell us which cuts of the amplitude have zero or non-zero support on the (boundary of the) amplituhedron.

Specifically, we propose a check that is motivated by the Cutkosky rules [21], which tell us that to compute the cut of an amplitude with respect to some set of cut con-

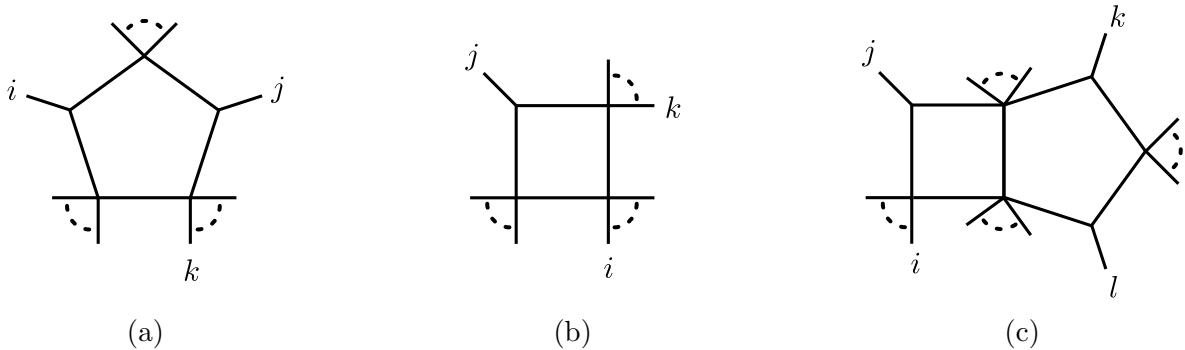


Figure 1: Three examples of cuts on which MHV amplitudes have no support; these appeared as spurious singularities in the Landau equation analysis of [17] since scalar pentagon and double pentagon integrals do have these cuts.

ditions, one replaces the on-shell propagators in the integrand corresponding to those cut conditions by delta-functions, and integrates the resulting quantity over the loop momenta. The result of such a calculation has a chance to be non-zero only if the locus where the cut conditions are all satisfied has non-trivial overlap with the domain of integration of the loop momentum variables. In the present context, that domain is the space of mutually positive lines, i.e., the interior of the amplituhedron. This principle will lead to a fundamental asymmetry between the two types of Landau equations in our analysis. The full set of Landau equations including both eqs. (1.9) and (1.10) should be solvable only on a codimension-one locus in the space of external momenta in order to obtain a valid branch point. However, guided by Cutkosky, we claim that the cut conditions (1.10) must be solvable inside the positive domain for arbitrary (positive) external kinematics; otherwise the discontinuity around the putative branch point is zero and we should discard it as spurious.

In the remainder of this section we will demonstrate this hypothesis by means of the examples shown in figure 1. The leading Landau singularities of each of these diagrams were found to be singularities of the scalar pentagon and double-pentagon integrals analyzed in [17], but it is clear that MHV amplitudes have no support on these cut configurations. In the next three subsections we will see how to understand their spuriousness directly from the amplituhedron. This will motivate us to seek a better, more direct algorithm to be presented in the following section.

2.1 The Spurious Pentagon Singularity

The first spurious singularity of MHV amplitudes arising from the integral representation used in [17] is the leading Landau singularity of the pentagon shown in figure 1a,

which is located on the locus where

$$\langle i j k k+1 \rangle \langle \bar{i} \cap \bar{j} k k+1 \rangle = 0. \quad (2.1)$$

It was noted already in [21] that this solution of the Landau equations does not correspond to a branch point of the pentagon integral. It arises from cut conditions that put all five propagators of the pentagon on-shell:

$$0 = \langle \mathcal{L} i-1 i \rangle = \langle \mathcal{L} i i+1 \rangle = \langle \mathcal{L} j-1 j \rangle = \langle \mathcal{L} j j+1 \rangle = \langle \mathcal{L} k k+1 \rangle, \quad (2.2)$$

where \mathcal{L} is the loop momentum. The first four of these cut conditions admit two discrete solutions [26]: either $\mathcal{L} = (i j)$ or $\mathcal{L} = \bar{i} \cap \bar{j}$. The second of these cannot avoid lying outside the amplituhedron. We see this by representing its D -matrix as

$$D = \begin{pmatrix} i-1 & i & i+1 \\ \langle i \bar{j} \rangle & -\langle i-1 \bar{j} \rangle & 0 \\ 0 & \langle i+1 \bar{j} \rangle & -\langle i \bar{j} \rangle \end{pmatrix}, \quad (2.3)$$

where we indicate only the nonzero columns of the $2 \times n$ matrix in positions $i-1$, i and $i+1$, per the labels above the matrix. The non-zero 2×2 minors of this matrix,

$$\langle i \bar{j} \rangle \langle i+1 \bar{j} \rangle, \quad \langle i-1 \bar{j} \rangle \langle i \bar{j} \rangle, \quad -\langle i \bar{j} \rangle^2 \quad (2.4)$$

have indefinite signs for general positive external kinematics, so this \mathcal{L} lies discretely outside the amplituhedron.

We proceed with the first solution $\mathcal{L} = (i j)$ which can be represented by the trivial D -matrix

$$D = \begin{pmatrix} i & j \\ 1 & 0 \\ 0 & 1 \end{pmatrix}. \quad (2.5)$$

Although this is trivially positive, upon substituting $\mathcal{L} = (i j)$ into eq. (2.2) we find that the fifth cut condition can only be satisfied for special kinematics satisfying

$$\langle i j k k+1 \rangle = 0. \quad (2.6)$$

Therefore, according to the Cutkosky-inspired rule discussed three paragraphs ago, the monodromy around this putative singularity vanishes for general kinematics and hence it is not a valid branch point at one loop. Indeed this conclusion is easily verified by looking at the explicit results of [33].

2.2 The Spurious Three-Mass Box Singularity

The second spurious one-loop singularity encountered in [17] is a subleading singularity of the pentagon which lives on the locus

$$\langle j(j-1 j+1)(i i+1)(k k+1) \rangle = 0 \quad (2.7)$$

and arises from the cut conditions shown in figure 1b:

$$0 = \langle \mathcal{L} i i+1 \rangle = \langle \mathcal{L} j-1 j \rangle = \langle \mathcal{L} j j+1 \rangle = \langle \mathcal{L} k k+1 \rangle. \quad (2.8)$$

These are of three-mass box type and have the two solutions [4]

$$\mathcal{L} = (j i i+1) \cap (j k k+1) \text{ or } \mathcal{L} = (\bar{j} \cap (i i+1), \bar{j} \cap (k k+1)). \quad (2.9)$$

The two solutions may be represented respectively by the D -matrices

$$D = \begin{pmatrix} & i & i+1 & j \\ & 0 & 0 & 1 \\ \langle i+1 j k k+1 \rangle & -\langle i j k k+1 \rangle & 0 & 0 \end{pmatrix} \quad (2.10)$$

and

$$D = \begin{pmatrix} & i & i+1 & k & k+1 \\ \langle i+1 \bar{j} \rangle & -\langle i \bar{j} \rangle & 0 & 0 & 0 \\ 0 & 0 & -\langle \bar{j} k+1 \rangle & \langle \bar{j} k \rangle & 0 \end{pmatrix}. \quad (2.11)$$

Neither matrix is non-negative definite when the Z 's are in the positive domain $G_+(4, n)$, so we again reach the (correct) conclusion that one-loop MHV amplitudes do not have singularities on the locus where eq. (2.7) is satisfied (for generic i, j and k).

2.3 A Two-Loop Example

The two-loop scalar double-pentagon integral considered in [17] has a large number of Landau singularities that are spurious singularities of two-loop MHV amplitudes. It would be cumbersome to start with the full list and eliminate the spurious singularities one at a time using the amplituhedron. Here we will be content to consider one example in detail before abandoning this approach in favor of one more directly built on the amplituhedron.

We consider the Landau singularities shown in eq. (4.12) of [17] which live on the locus

$$\langle j(j-1 j+1)(i-1 i)(k l) \rangle \langle j(j-1 j+1)(i-1 i) \bar{k} \cap \bar{l} \rangle = 0. \quad (2.12)$$

We consider the generic case when the indices i, j, k, l are well-separated; certain degenerate cases do correspond to non-spurious singularities. This singularity is of

pentagon-box type shown in figure 1c since it was found in [17] to arise from the eight cut conditions

$$\begin{aligned}\langle \mathcal{L}^{(1)} i-1 i \rangle &= \langle \mathcal{L}^{(1)} j-1 j \rangle = \langle \mathcal{L}^{(1)} j j+1 \rangle = \langle \mathcal{L}^{(1)} \mathcal{L}^{(2)} \rangle = 0, \\ \langle \mathcal{L}^{(2)} k-1 k \rangle &= \langle \mathcal{L}^{(2)} k k+1 \rangle = \langle \mathcal{L}^{(2)} l-1 l \rangle = \langle \mathcal{L}^{(2)} ll+1 \rangle = 0.\end{aligned}\tag{2.13}$$

The last four equations have two solutions $\mathcal{L}^{(2)} = (kl)$ or $\mathcal{L}^{(2)} = \bar{k} \cap \bar{l}$, but as in the previous subsection, only the first of these has a chance to avoid being outside the amplituhedron. Taking $\mathcal{L}^{(2)} = (kl)$, the two solutions to the first four cut conditions are then

$$\mathcal{L}^{(1)} = (j i-1 i) \cap (j k l) = (Z_j, Z_{i-1} \langle i j k l \rangle - Z_i \langle i-1 j k l \rangle) \text{ or}\tag{2.14}$$

$$\mathcal{L}^{(1)} = \left((i-1 i) \cap \bar{j}, (k l) \cap \bar{j} \right) = \left(Z_{i-1} \langle i \bar{j} \rangle - Z_i \langle i-1 \bar{j} \rangle, Z_k \langle l \bar{j} \rangle - Z_l \langle k \bar{j} \rangle \right).\tag{2.15}$$

The D -matrices corresponding to the first solution can be taken as

$$\begin{pmatrix} D^{(1)} \\ D^{(2)} \end{pmatrix} = \begin{pmatrix} i-1 & i & j & k & l \\ 0 & 0 & 1 & 0 & 0 \\ \langle i j k l \rangle & -\langle i-1 j k l \rangle & 0 & 0 & 0 \\ 0 & 0 & 0 & 1 & 0 \\ 0 & 0 & 0 & 0 & 1 \end{pmatrix}.\tag{2.16}$$

Evidently two of its 4×4 minors are $-\langle i j k l \rangle$ and $\langle i-1 j k l \rangle$, which have opposite signs for generic Z in the positive domain. D -matrices corresponding to the second solution can be written as

$$\begin{pmatrix} D^{(1)} \\ D^{(2)} \end{pmatrix} = \begin{pmatrix} i-1 & i & k & l \\ \langle i \bar{j} \rangle & -\langle i-1 \bar{j} \rangle & 0 & 0 \\ 0 & 0 & \langle l \bar{j} \rangle & -\langle k \bar{j} \rangle \\ 0 & 0 & 1 & 0 \\ 0 & 0 & 0 & 1 \end{pmatrix},\tag{2.17}$$

which again has minors of opposite signs.

We conclude that the locus where the cut conditions (2.13) are satisfied lies strictly outside the amplituhedron, and therefore that there is no discontinuity around the putative branch point at (2.12). Indeed, this is manifested by the known fact [34] that two-loop MHV amplitudes do not have symbol entries which vanish on this locus. Actually, while correct, we were slightly too hasty in reaching this conclusion, since we only analyzed one set of cut conditions. Although it doesn't happen in this example, in general there may exist several different collections of cut conditions associated to the same Landau singularity, and the discontinuity around that singularity would receive additive contributions from each distinct set of associated cut contributions.

2.4 Summary

We have shown, via a slight refinement of the analysis carried out in [17], that the spurious branch points of one- and two-loop MHV amplitudes encountered in that paper can be eliminated simply on the basis of positivity constraints in the amplituhedron. It is simple to see that the cuts considered above have no support for MHV amplitudes so it may seem like overkill to use the fancy language of the amplituhedron. However we wanted to highlight the following approach:

(1) First, consider a representation of an amplitude as a sum over a particular type of Feynman integrals. Find the Landau singularities of a generic term in the sum. These tell us the loci in Z -space where the amplitude *may* have a singularity.

(2) For each *potential* singularity obtained in (1), check whether the corresponding on-shell conditions have a non-zero intersection with the (closure of) the amplituhedron. If the answer is no, for all possible sets of cut conditions associated with a given Landau singularity, then the singularity must be spurious.

This approach is conceptually straightforward but inefficient. One manifestation of this inefficiency is that although double pentagon integrals are characterized by four free indices i, j, k, l , we will see in the next section the vast majority of the resulting potential singularities are spurious. Specifically we will see that in order for the solution to a given set of cut conditions to have support inside the (closure of) the amplituhedron, the conditions must be relaxed in such a way that they involve only three free indices. In other words, most of the $\mathcal{O}(n^4)$ singularities of individual double pentagon integrals must necessarily cancel out when they are summed, leaving only $\mathcal{O}(n^3)$ physical singularities of the full two-loop MHV amplitudes. (The fact that these amplitudes have only $\mathcal{O}(n^3)$ singularities is manifest in the result of [34].) This motivates us to seek a more “amplituhedrony” approach to finding singularities where we do not start by considering any particular representation of the amplitude, but instead start by thinking directly about positive configurations of loops $\mathcal{L}^{(\ell)}$.

3 An Amplituhedrony Approach

The most significant drawback of the approach taken in the previous section is that it relies on having explicit representations of an integrand in terms of local Feynman integrals. These have been constructed for all two-loop amplitudes in SYM theory [35], but at higher loop order even finding such representations becomes a huge computational challenge that we would like to be able to bypass. Also, as the loop order increases, the number of potential Landau singularities grows rapidly, and the vast majority of

these potential singularities will fail the positivity analysis and hence turn out to be spurious. We would rather not have to sift through all of this chaff to find the wheat.

Let’s begin by taking a step back to appreciate that the only reason we needed the crutch of local Feynman integrals in the previous section is that each Feynman diagram topology provides a set of propagators for which we can solve the associated Landau equations (1.9) and (1.10) to find potential singularities. Then, for each set of cut conditions, we can determine whether the associated Landau singularity is physical or spurious by asking the amplituhedron whether or not the set of loops $\mathcal{L}^{(\ell)}$ satisfying the cut conditions has any overlap with the amplituhedron.

In this section we propose a more “amplituhedrony” approach that does not rely on detailed knowledge of integrands. We invert the logic of the previous section: instead of using Feynman diagrams to generate sets of cut conditions that we need to check one by one, we can ask the amplituhedron itself to directly identify all potentially “valid” sets of cut conditions that are possibly relevant to the singularities of an amplitude.

To phrase the problem more abstractly: for a planar n -particle amplitude at L -loop order, there are in general $nL + L(L - 1)/2$ possible local cut conditions one can write down:

$$\langle \mathcal{L}^{(\ell)} i i+1 \rangle = 0 \text{ for all } \ell, i \text{ and } \langle \mathcal{L}^{(\ell_1)} \mathcal{L}^{(\ell_2)} \rangle = 0 \text{ for all } \ell_1 \neq \ell_2. \quad (3.1)$$

We simply need to characterize which subsets of these cut conditions can possibly be simultaneously satisfied for loop momenta $\mathcal{L}^{(\ell)}$ living in the closure of the amplituhedron. Each such set of cut conditions is a subset of one or more maximal subsets, and these maximal subsets are just the maximal codimension boundaries of the amplituhedron.

Fortunately, the maximal codimension boundaries of the MHV amplituhedron are particularly simple, as explained in [5]. Each loop momentum $\mathcal{L}^{(\ell)}$ must take the form $(i j)$ for some i and j (that can be different for different ℓ), and the condition of mutual positivity enforces an emergent planarity: if all of the lines $\mathcal{L}^{(\ell)}$ are drawn as chords on a disk between points on the boundary labeled $1, 2, \dots, n$, then positivity forbids any two lines to cross in the interior of the disk. In what follows we follow a somewhat low-brow analysis in which we systematically consider relaxations away from the maximum codimension boundaries, but the procedure can be streamlined by better harnessing this emergent planarity, which certainly pays off at higher loop order [36].

In the next few subsections we demonstrate this “amplituhedrony” approach explicitly at one and two loops before summarizing the main idea at the end of the section.

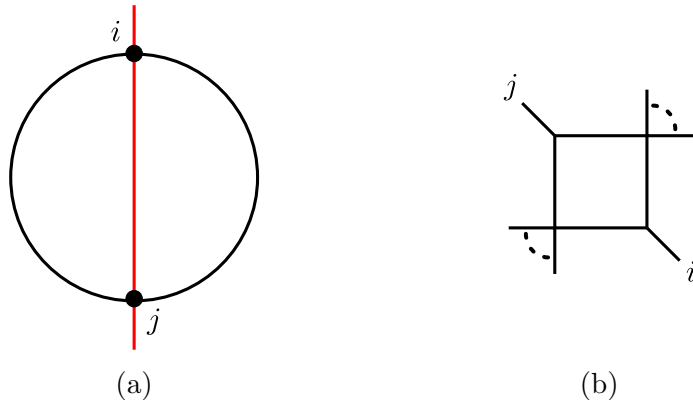


Figure 2: (a) A maximum codimension boundary of the one-loop MHV amplituhedron. The circle is a schematic depiction of the n line segments $(12), (23), \dots, (n1)$ connecting the n cyclically ordered external kinematic points $Z_i \in G_+(4, n)$ and the red line shows the loop momentum $\mathcal{L} = (ij)$. (b) The corresponding Landau diagram, which is a graphical depiction of the four cut conditions (3.3) that are satisfied on this boundary.

3.1 One-Loop MHV Amplitudes

The maximum codimension boundaries of the one-loop MHV amplituhedron occur when

$$\mathcal{L} = (ij), \quad (3.2)$$

as depicted in figure 2a. On this boundary four cut conditions of “two-mass easy” type [33] are manifestly satisfied:

$$\langle \mathcal{L} i-1 i \rangle = \langle \mathcal{L} i i+1 \rangle = \langle \mathcal{L} j-1 j \rangle = \langle \mathcal{L} j j+1 \rangle = 0, \quad (3.3)$$

as depicted in the Landau diagram shown in figure 2b. (For the moment we consider i and j to be well separated so there are no accidental degenerations.) The Landau analysis of eq. (3.3) has been performed long ago [20, 28] and reviewed in the language of momentum twistors in [17]. A leading solution to the Landau equations exists only if

$$\langle i \bar{j} \rangle \langle \bar{i} j \rangle = 0. \quad (3.4)$$

Subleading Landau equations are obtained by relaxing one of the four on-shell conditions. This leads to cuts of two-mass triangle type, which are uninteresting (they exist for generic kinematics, so don’t correspond to branch points of the amplitude). At sub-subleading order we reach cuts of bubble type. For example if we relax the

second and fourth condition in eq. (3.3) then we encounter a Landau singularity which lives on the locus

$$\langle i-1 \ i \ j-1 \ j \rangle = 0. \quad (3.5)$$

Other relaxations either give no constraint on kinematics, or the same as eq. (3.5) with $i \rightarrow i+1$ and/or $j \rightarrow j+1$.

Altogether, we reach the conclusion that all physical branch points of one-loop MHV amplitudes occur on loci of the form

$$\langle a \ \bar{b} \rangle = 0 \text{ or } \langle a \ a+1 \ b \ b+1 \rangle = 0 \quad (3.6)$$

for various a, b . (Note that whenever we say there is a branch point at $x = 0$, we mean more specifically that there is a branch cut between $x = 0$ and $x = \infty$.) Indeed, these exhaust the branch points of the one-loop MHV amplitudes (first computed in [33]) except for branch points arising as a consequence of infrared regularization, which are captured by the BDS ansatz [37].

3.2 Two-Loop MHV Amplitudes: Configurations of Positive Lines

We divide the two-loop analysis into two steps. First, in this subsection, we classify valid configurations of mutually non-negative lines. This provides a list of the sets of cut conditions on which two-loop MHV amplitudes have nonvanishing support. Then in the following subsection we solve the Landau equations for each set of cut conditions, to find the actual location of the corresponding branch point.

At two loops the MHV amplituhedron has two distinct kinds of maximum codimension boundaries [5]. The first type has $\mathcal{L}^{(1)} = (i \ j)$ and $\mathcal{L}^{(2)} = (k \ l)$ for distinct cyclically ordered i, j, k, l . Since $\langle \mathcal{L}^{(1)} \ \mathcal{L}^{(2)} \rangle$ is non-vanishing (inside the positive domain $G_+(4, n)$) in this case, this boundary can be thought of as corresponding to a cut of a product of one-loop Feynman integrals, with no common propagator $\langle \mathcal{L}^{(1)} \ \mathcal{L}^{(2)} \rangle$. Therefore we will not learn anything about two-loop singularities beyond what is already apparent at one loop.

The more interesting type of maximum codimension boundary has $\mathcal{L}^{(1)} = (i \ j)$ and $\mathcal{L}^{(2)} = (i \ k)$, as depicted in figure 3a. Without loss of generality $i < j < k$, and for now we will moreover assume that i, j and k are well-separated to avoid any potential degenerations. (These can be relaxed at the end of the analysis, in particular to see that the degenerate case $j = k$ gives nothing interesting.) On this boundary the following nine cut conditions shown in the Landau diagram of figure 3b

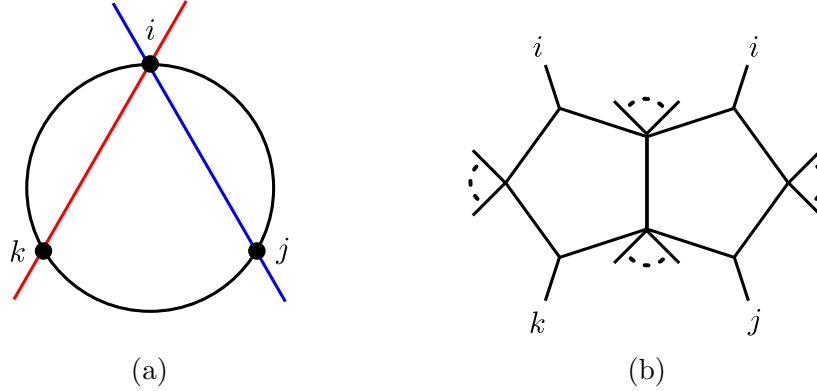


Figure 3: (a) A maximum codimension boundary of the two-loop MHV amplituhedron. (b) The corresponding Landau diagram (which, it should be noted, does not have the form of a standard Feynman integral) depicting the nine cut conditions (3.7)–(3.9) that are satisfied on this boundary.

are simultaneously satisfied:

$$\langle \mathcal{L}^{(1)} i-1 i \rangle = \langle \mathcal{L}^{(1)} i i+1 \rangle = \langle \mathcal{L}^{(2)} i-1 i \rangle = \langle \mathcal{L}^{(2)} i i+1 \rangle = 0, \quad (3.7)$$

$$\langle \mathcal{L}^{(1)} j-1 j \rangle = \langle \mathcal{L}^{(1)} j j+1 \rangle = \langle \mathcal{L}^{(2)} k-1 k \rangle = \langle \mathcal{L}^{(2)} k k+1 \rangle = 0, \quad (3.8)$$

$$\langle \mathcal{L}^{(1)} \mathcal{L}^{(2)} \rangle = 0. \quad (3.9)$$

This is the maximal set of cuts that can be simultaneously satisfied while keeping the $\mathcal{L}^{(\ell)}$'s inside the closure of the amplituhedron for generic $Z \in G_+(4, n)$. We immediately note that since only three free indices i, j, k are involved, this set of cuts manifestly has size $\mathcal{O}(n^3)$, representing immediate savings compared to the larger $\mathcal{O}(n^4)$ set of double-pentagon cut conditions as discussed at the end of the previous section.

We can generate other, smaller sets of cut conditions by relaxing some of the nine shown in eqs. (3.7)–(3.9). This corresponds to looking at subleading singularities, in the language of the Landau equations. However, it is not interesting to consider relaxations that lead to $\langle \mathcal{L}^{(1)} \mathcal{L}^{(2)} \rangle \neq 0$ because, as mentioned above, it essentially factorizes the problem into a product of one-loop cuts. Therefore in what follows we only consider cuts on which $\langle \mathcal{L}^{(1)} \mathcal{L}^{(2)} \rangle = 0$.

By relaxing various subsets of the other 8 conditions we can generate 2^8 subsets of cut conditions. In principle each subset should be analyzed separately, but there is clearly a natural stratification of relaxations which we can exploit to approach the problem systematically. In fact, we will see that the four cut conditions in eq. (3.7) that involve the point i play a special role. Specifically, we will see that the four cut conditions in eq. (3.8) involving j and k can always be relaxed, or un-relaxed, “for free”,

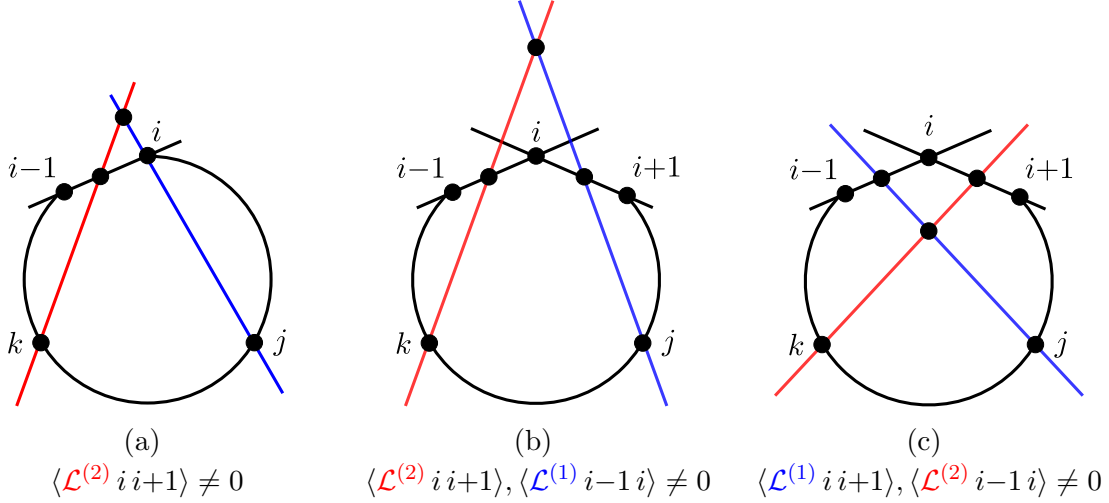


Figure 4: Three different invalid relaxations of the maximal codimension boundary shown in figure 3.

with no impact on positivity. Therefore, we see that whether a configuration of loops may be positive or not depends only on which subset of the four cut conditions (3.7) is relaxed.

In this subsection we will classify the subsets of eq. (3.7) that lead to valid configurations of positive lines $\mathcal{L}^{(\ell)}$, and in the next subsection we will find the locations of the corresponding Landau singularities.

Relaxing none of eq. (3.7) [figure 3a]. At maximum codimension we begin with the obviously valid pair of mutually non-negative lines represented trivially by

$$\begin{pmatrix} D^{(1)} \\ D^{(2)} \end{pmatrix} = \begin{pmatrix} i & j & k \\ 1 & 0 & 0 \\ 0 & 1 & 0 \\ 1 & 0 & 0 \\ 0 & 0 & 1 \end{pmatrix}. \quad (3.10)$$

Relaxing any one of eq. (3.7). The four cases are identical up to relabeling so we consider relaxing the condition $\langle \mathcal{L}^{(2)} i i+1 \rangle = 0$, shown in figure 4a. In this case the remaining seven cut conditions on the first two lines of eqs. (3.7) and (3.8) admit the one-parameter family of solutions

$$\mathcal{L}^{(1)} = (i j), \quad \mathcal{L}^{(2)} = (Z_k, \alpha Z_{i-1} + (1 - \alpha) Z_i). \quad (3.11)$$

We recall that the parity conjugate solutions having $\mathcal{L}^{(1)} = \bar{i} \cap \bar{j}$ lie discretely outside the amplituhedron as seen in eq. (2.3). The corresponding D -matrices

$$\begin{pmatrix} D^{(1)} \\ D^{(2)} \end{pmatrix} = \begin{pmatrix} i-1 & i & j & k \\ 0 & 1 & 0 & 0 \\ 0 & 0 & 1 & 0 \\ \alpha & 1-\alpha & 0 & 0 \\ 0 & 0 & 0 & 1 \end{pmatrix} \quad (3.12)$$

are mutually non-negative for $0 \leq \alpha \leq 1$. It remains to impose the final cut condition that $\mathcal{L}^{(1)}$ and $\mathcal{L}^{(2)}$ intersect:

$$\langle \mathcal{L}^{(1)} \mathcal{L}^{(2)} \rangle = \alpha \langle i-1 \ i \ j \ k \rangle = 0. \quad (3.13)$$

For general positive external kinematics this will only be satisfied when $\alpha = 0$, which brings us back to the maximum codimension boundary. We conclude that the loop configurations of this type do not generate branch points.

Relaxing $\langle \mathcal{L}^{(1)} i-1 \ i \rangle = 0$ **and** $\langle \mathcal{L}^{(2)} \ i \ i+1 \rangle = 0$ [figure 4b]. In this case the six remaining cut conditions in eqs. (3.7) and (3.8) admit the two-parameter family of solutions

$$\mathcal{L}^{(1)} = (\alpha Z_i + (1-\alpha)Z_{i+1}, Z_j), \quad \mathcal{L}^{(2)} = (\beta Z_i + (1-\beta)Z_{i-1}, Z_k). \quad (3.14)$$

The corresponding D -matrices

$$\begin{pmatrix} D^{(1)} \\ D^{(2)} \end{pmatrix} = \begin{pmatrix} i-1 & i & i+1 & j & k \\ 0 & \alpha & 1-\alpha & 0 & 0 \\ 0 & 0 & 0 & 1 & 0 \\ 1-\beta & \beta & 0 & 0 & 0 \\ 0 & 0 & 0 & 0 & 1 \end{pmatrix} \quad (3.15)$$

are mutually non-negative if $0 \leq \alpha, \beta \leq 1$. Imposing that the two loops intersect gives the constraint

$$\langle \mathcal{L}^{(1)} \mathcal{L}^{(2)} \rangle = \alpha(1-\beta) \langle i-1 \ i \ j \ k \rangle + (1-\alpha)\beta \langle i \ i+1 \ j \ k \rangle + (1-\alpha)(1-\beta) \langle i-1 \ i+1 \ j \ k \rangle = 0, \quad (3.16)$$

which is not satisfied for general positive kinematics unless $\alpha = \beta = 1$, which again brings us back to the maximum codimension boundary.

Relaxing the two conditions $\langle \mathcal{L}^{(1)} \ i \ i+1 \rangle = \langle \mathcal{L}^{(2)} \ i \ i-1 \rangle = 0$, depicted in figure 4c, is easily seen to lead to the same conclusion.

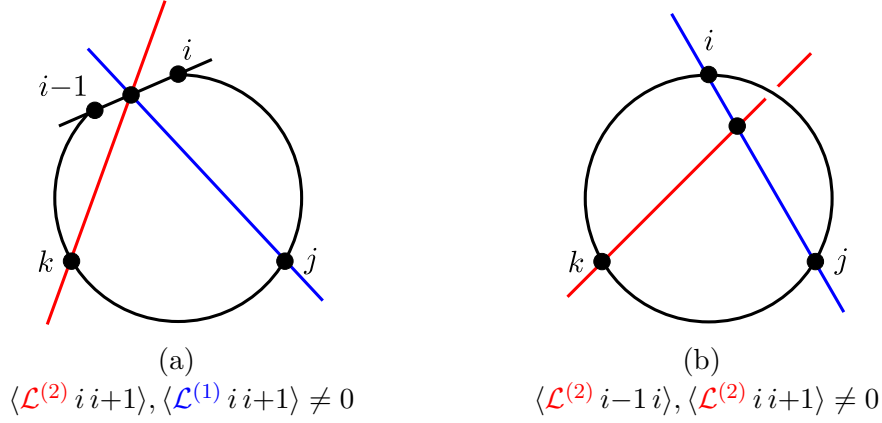


Figure 5: Two valid double relaxations of figure 3. The other two possibilities are obtained by taking $i \rightarrow i+1$ in (a) or $\mathcal{L}^{(2)} \rightarrow \mathcal{L}^{(1)}$ and $j \leftrightarrow k$ in (b).

Relaxing $\langle \mathcal{L}^{(1)} i i+1 \rangle = 0$ and $\langle \mathcal{L}^{(2)} i i+1 \rangle = 0$ [figure 5a]. In this case there is a one-parameter family of solutions satisfying all seven remaining cut conditions including $\langle \mathcal{L}^{(1)} \mathcal{L}^{(2)} \rangle = 0$:

$$\mathcal{L}^{(1)} = (\alpha Z_i + (1 - \alpha) Z_{i+1}, Z_j), \quad \mathcal{L}^{(2)} = (\alpha Z_i + (1 - \alpha) Z_{i+1}, Z_k). \quad (3.17)$$

The D -matrices can be represented as

$$\begin{pmatrix} D^{(1)} \\ D^{(2)} \end{pmatrix} = \begin{pmatrix} i & i+1 & j & k \\ \alpha & 1 - \alpha & 0 & 0 \\ 0 & 0 & 1 & 0 \\ \alpha & 1 - \alpha & 0 & 0 \\ 0 & 0 & 0 & 1 \end{pmatrix}, \quad (3.18)$$

which is a valid mutually non-negative configuration for $0 \leq \alpha \leq 1$. We conclude that these configurations represent physical branch points of two-loop MHV amplitudes by appealing to Cutkosian intuition, according to which we would compute the discontinuity of the amplitude around this branch point by integrating over $0 \leq \alpha \leq 1$ (in figure 5a this corresponds to integrating the intersection point of the two \mathcal{L} 's over the line segment between Z_{i-1} and Z_i).

Relaxing the two conditions $\langle \mathcal{L}^{(1)} i i-1 \rangle = \langle \mathcal{L}^{(2)} i i-1 \rangle = 0$ is clearly equivalent up to relabeling.

Relaxing $\langle \mathcal{L}^{(2)} i-1 i \rangle = 0$ and $\langle \mathcal{L}^{(2)} i i+1 \rangle = 0$ [figure 5b]. The seven remaining cut conditions admit a one-parameter family of solutions

$$\mathcal{L}^{(1)} = (i j), \quad \mathcal{L}^{(2)} = (\alpha Z_i + (1 - \alpha) Z_j, Z_k), \quad (3.19)$$

which can be represented by

$$\begin{pmatrix} D^{(1)} \\ D^{(2)} \end{pmatrix} = \begin{pmatrix} i & j & k \\ 1 & 0 & 0 \\ 0 & 1 & 0 \\ \alpha & 1 - \alpha & 0 \\ 0 & 0 & 1 \end{pmatrix}. \quad (3.20)$$

This is a valid configuration of mutually non-negative lines for $0 \leq \alpha \leq 1$ so we expect it to correspond to a physical branch point. Clearly the same conclusion holds if we were to completely relax $\mathcal{L}^{(1)}$ at i instead of $\mathcal{L}^{(2)}$.

Higher relaxations of eq. (3.7). So far we have considered the relaxation of any one or any two of the conditions shown in eq. (3.7). We have found that single relaxations do not yield branch points of the amplitude, and that four of the six double relaxations are valid while the two double relaxations shown in figures 4b and 4c are invalid.

What about triple relaxations? These can be checked by explicit construction of the relevant D -matrices, but it is also easy to see graphically that any triple relaxation is valid because they can all be reached by relaxing one of the valid double relaxations. For example, the triple relaxation where we relax all of eq. (3.7) except $\langle \mathcal{L}^{(1)} i-1 i \rangle = 0$ can be realized by rotating $\mathcal{L}^{(2)}$ in figure 5a clockwise around the point k so that it continues to intersect $\mathcal{L}^{(1)}$. As a second example, the triple relaxation where we relax all but $\langle \mathcal{L}^{(2)} i-1 i \rangle = 0$ can be realized by rotating $\mathcal{L}^{(1)}$ in figure 5a counter-clockwise around the point j so that it continues to intersect $\mathcal{L}^{(2)}$.

Finally we turn to the case when all four cut conditions in eq. (3.7) are relaxed. These relaxed cut conditions admit two branches of solutions, represented by D -matrices of the form

$$\begin{pmatrix} D^{(1)} \\ D^{(2)} \end{pmatrix} = \begin{pmatrix} j & j+1 & \cdots & k-1 & k \\ 1 & 0 & \cdots & 0 & 0 \\ \alpha_j & \alpha_{j+1} & \cdots & \alpha_{k-1} & \alpha_k \\ \alpha_j & \alpha_{j+1} & \cdots & \alpha_{k-1} & \alpha_k \\ 0 & 0 & \cdots & 0 & 1 \end{pmatrix} \quad (3.21)$$

or a similar form with α parameters wrapping the other way around from k to j :

$$\begin{pmatrix} D^{(1)} \\ D^{(2)} \end{pmatrix} = \begin{pmatrix} \cdots & j-1 & j & k & k+1 & \cdots \\ \cdots & \alpha_{j-1} & \alpha_j & -\alpha_k & -\alpha_{k+1} & \cdots \\ \cdots & 0 & 1 & 0 & 0 & \cdots \\ \cdots & \alpha_{j-1} & \alpha_j & -\alpha_k & -\alpha_{k+1} & \cdots \\ \cdots & 0 & 0 & 1 & 0 & \cdots \end{pmatrix}. \quad (3.22)$$

Both of these parameterize valid configuration of mutually non-negative lines as long as all of the α 's are positive.

Relaxing $\mathcal{L}^{(1)}$ at j and/or $\mathcal{L}^{(2)}$ at k . All of the configurations we have considered so far keep the four propagators in eq. (3.8) on shell. However it is easy to see that none of these conditions have any bearing on positivity one way or the other. For example, there is no way to render the configuration shown in figure 4b positive by moving $\mathcal{L}^{(1)}$ away from the vertex j while maintaining all of the other cut conditions. On the other hand, there is no way to spoil the positivity of the configuration shown in figure 5b by moving $\mathcal{L}^{(2)}$ away from the vertex k while maintaining all other cut conditions.

Summary. We call a set of cut conditions “valid” if the $m \geq 0$ -dimensional locus in \mathcal{L} -space where the conditions are simultaneously satisfied has non-trivial m -dimensional overlap with the closure of the amplituhedron. (The examples shown in figures 5a and 5b both have $m = 1$, but further relaxations would have higher-dimensional solution spaces.) As mentioned above, this criterion is motivated by Cutkoskian intuition that the discontinuity of the amplitude would be computed by an integral over the intersection of this locus with the (closure of the) amplituhedron. If this intersection is empty (or lives on a subspace that is less than m -dimensional) then such an integral would vanish, signalling that the putative singularity is actually spurious.

The nine cut conditions shown in eqs. (3.7)–(3.9) are solved by the configuration of lines shown in figure 3a that is a zero-dimensional boundary of the amplituhedron. We have systematically investigated relaxing various subsets of these conditions (with the exception of eq. (3.9), to stay within the realm of genuine two-loop singularities) to determine which relaxations are “valid” in the sense just described.

Conclusion: The most general valid relaxation of the configuration shown in figure 3a is either an arbitrary relaxation at the points j and k , or an arbitrary relaxation of figure 5a (or the same with $i \mapsto i+1$), or an arbitrary relaxation of figure 5b (or the same with $j \leftrightarrow k$). The configurations shown in figure 4, and further relaxations thereof that are not relaxations of those shown in figure 5, are invalid.

3.3 Two-Loop MHV Amplitudes: Landau Singularities

In the previous subsection we asked the amplituhedron directly to tell us which possible sets of cut conditions are valid for two-loop MHV amplitudes, rather than starting from some integral representation and using the amplituhedron to laboriously sift through the many spurious singularities. We can draw Landau diagrams for each valid relaxation to serve as a graphical indicator of the cut conditions that are satisfied. The Landau diagram with nine propagators corresponding to the nine cut conditions satisfied by

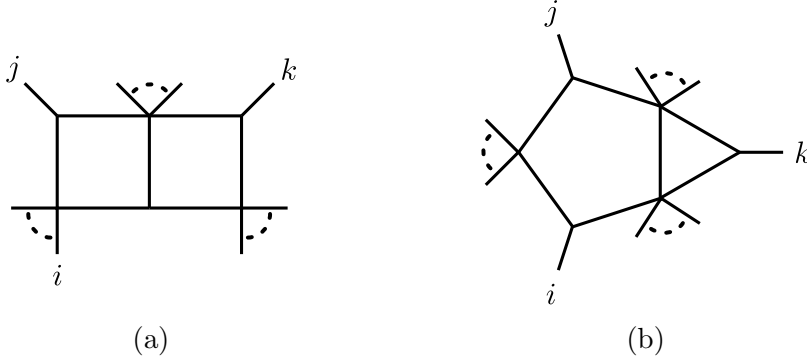


Figure 6: The Landau diagrams showing the seven cut conditions satisfied by figures 5a and 5b, respectively.

figure 3a was already displayed in figure 3b. The configurations shown in figures 5a and 5b satisfy the seven cut conditions corresponding to the seven propagators in figures 6a and 6b, respectively. We are now ready to determine the locations of the branch points associated to these valid cut configurations (and their relaxations) by solving the Landau equations.

The following calculations follow very closely those done in [17]. Note that throughout this section, in solving cut conditions we will always ignore branches of solutions (for example those of the type $\mathcal{L} = \bar{i} \cap \bar{j}$) which cannot satisfy positivity.

The double-box. For the double-box shown in in figure 6a let us use $A \in \mathbb{P}^3$ to denote the point on the line $(i-1, i)$ where the two loop lines $\mathcal{L}^{(\ell)}$ intersect. These can then be parameterized as $\mathcal{L}^{(1)} = (A, Z_j)$ and $\mathcal{L}^{(2)} = (A, Z_k)$. The quickest way to find the location of the leading Landau singularity is to impose eq. (1.9) for each of the two loops. These are both of two-mass easy type, so we find that the Landau singularity lives on the locus (see [17])

$$\langle i-1 \ i \ j \ k \rangle \langle A \bar{j} \rangle = \langle i-1 \ i \ j \ k \rangle \langle A \bar{k} \rangle = 0. \quad (3.23)$$

These can be solved in two ways; either by

$$\langle i-1 \ i \ j \ k \rangle = 0 \quad (3.24)$$

or by solving the first condition for $A = \bar{j} \cap (i-1 \ i)$ and substituting this into the second condition to find

$$\langle i-1 \ i \ \bar{j} \cap \bar{k} \rangle = 0. \quad (3.25)$$

The astute reader may recall that in (2.6) we discarded a singularity of the same type as in eq. (3.24). This example highlights that it is crucial to appreciate the

essential asymmetry between the roles of the two types of Landau equations. The on-shell conditions (1.9) by themselves only provide information about *discontinuities*. We discarded eq. (2.6) because the solution has support on a set of measure zero inside the closure of the amplituhedron, signalling that there is no discontinuity around the branch cut associated to the cut conditions shown in eq. (2.1). Therefore we never needed to inquire as to the actual location where the corresponding branch point might have been. To learn about the *location* of a branch point we have to solve also the second type of Landau equations (1.10). Indeed (3.24) does correspond to a branch point that lies outside the positive domain, but we don't discard it because the discontinuity of the amplitude around this branch point is nonzero. As mentioned above, according to the Cutkosky rules it would be computed by an integral over the line segment between Z_{i-1} and Z_i in figure 5a. When branch points lie outside $G_+(4, n)$, as in this case, it signals a discontinuity that does not exist on the physical sheet but on some other sheet; see the comments near the end of section 1.

Additional (sub k -leading, for various k) Landau singularities are exposed by setting various sets of α 's to zero in the Landau equations and relaxing the associated cut conditions. Although these precise configurations were not analyzed in [17], the results of that paper, together with some very useful tricks reviewed in appendix A, are easily used to reveal branch points at the loci

$$\langle j(j-1, j+1)(k, k\pm 1)(i-1, i) \rangle = 0 \tag{3.26}$$

together with the same for $j \leftrightarrow k$, as well as $\langle a a+1 b b+1 \rangle = 0$ for a, b drawn from the set $\{i-1, j-1, j, k-1, k\}$.

The pentagon-triangle. With the help of appendix A and the results of [17] it is easily seen that the leading singularity of the pentagon-triangle shown in figure 6b is located on the locus where

$$\langle i\bar{j} \rangle \langle \bar{i}j \rangle = 0. \tag{3.27}$$

The computation of additional singularities essentially reduces to the same calculation for a three-mass pentagon, which was carried out in [17]. Altogether we find that

branch points live on the loci

$$\begin{aligned}
\langle i j k-1 k \rangle &= 0, \\
\langle i(i-1 i+1)(j-1 j)(k-1 k) \rangle &= 0, \\
\langle i(i-1 i+1)(j j+1)(k-1 k) \rangle &= 0, \\
\langle j(j-1 j+1)(i-1 i)(k-1 k) \rangle &= 0, \\
\langle j(j-1 j+1)(i i+1)(k-1 k) \rangle &= 0, \\
\langle i i \pm 1 j k \rangle &= 0, \\
\langle i j j \pm 1 k \rangle &= 0,
\end{aligned} \tag{3.28}$$

together with the same collection with $(k-1 k) \rightarrow (k k+1)$, as well as all $\langle a a+1 b b+1 \rangle = 0$ for a, b drawn from the set $\{i-1, i, j-1, j, k-1, k\}$.

The maximum codimension boundaries. We left this case for last because it is somewhat more subtle. It is known that the final entries of the symbols of MHV amplitudes always have the form $\langle a \bar{b} \rangle$ [34]. We expect the leading Landau singularity of the maximum codimension boundary to expose branch points at the vanishing loci of these final entries.

However, if we naively solve the Landau equations for the diagram shown in 3b, we run into a puzzle. The first type of Landau equations (1.9) correspond to the nine cut conditions (3.7)–(3.9), which of course are satisfied by $\mathcal{L}^{(1)} = (i j)$ and $\mathcal{L}^{(2)} = (i k)$. The second type of Landau equations (1.10) does not impose any constraints for pentagons because it is always possible to find a vanishing linear combination of the five participating four-vectors. This naive Landau analysis therefore suggests that there is no leading branch point associated to the maximum codimension boundary.

This analysis is questionable because, as already noted above, the Landau diagram associated to the maximal codimension boundary, shown in figure (2b), does not have the form of a valid Feynman diagram. Therefore it makes little sense to trust the associated Landau analysis. Instead let us note that the nine cut conditions (3.7)–(3.9) are not independent; indeed they cannot be as there are only eight degrees of freedom in the loop momenta.

We are therefore motivated to identify which of the nine cut conditions (1) is redundant, in the sense that it is implied by the other eight for generic external kinematics, and (2) has the property that when omitted, the Landau diagram for the remaining eight takes the form of a valid planar Feynman diagram. None of the conditions involving j and k shown in eq. (3.8) are redundant; all of them must be imposed to stay on the maximum codimension boundary. The remaining five conditions in eqs. (3.7) and (3.9) are redundant for general kinematics, but only two of them satisfy the second property.

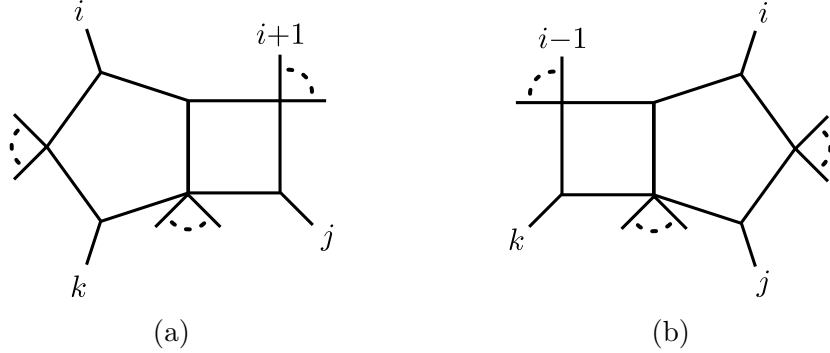


Figure 7: Landau diagrams corresponding to all of the cut conditions (3.7)–(3.9) except for (a) $\langle \mathcal{L}^{(1)} i-1 i \rangle = 0$, and (b) $\langle \mathcal{L}^{(2)} i i+1 \rangle = 0$. These are the only two cut conditions that are redundant (each is implied by the other eight, for generic kinematics) and, when omitted, lead to Landau diagrams that have the form of a standard Feynman integral. (In both figures $\mathcal{L}^{(1)}$ is the momentum in the right loop and $\mathcal{L}^{(2)}$ is the momentum in the left loop.)

The corresponding Landau diagrams are shown in fig. 7. Being valid planar Feynman diagrams, the integrand definitely receives contributions with these topologies (unlike fig. 2b), and will exhibit the associated Landau singularities.

It remains to compute the location of the leading Landau singularities for these diagrams. For fig. 7a the on-shell conditions for the pentagon set $\mathcal{L}^{(2)} = (i k)$ while the Kirkhoff condition for the box is

$$0 = \langle j (j-1 j+1) \mathcal{L}^{(2)}(i i+1) \rangle = \langle i \bar{j} \rangle \langle i i+1 j k \rangle. \quad (3.29)$$

The Landau equations associated to this topology therefore have solutions when $\langle i \bar{j} \rangle = 0$ or when $\langle i i+1 j k \rangle = 0$. However, on the locus $\langle i i+1 j k \rangle = 0$ it is no longer true that the eight on-shell conditions shown in fig. 7a imply the ninth condition $\langle \mathcal{L}^{(1)} i-1 i \rangle = 0$. Therefore, this solution of the Landau equations is not relevant to the maximum codimension boundary.

We conclude that the leading Landau singularity of the maximum codimension boundary is located on the locus where $\langle i \bar{j} \rangle = 0$ or (from fig. 7b) $\langle i \bar{k} \rangle = 0$. These results are in agreement with our expectation about the final symbol entries of MHV amplitudes [34]. Relaxations of Figures 7a, 7b at j, k will not produce any symbol entries.

Conclusion. In conclusion, our analysis has revealed that two-loop MHV amplitudes have physical branch points on the loci of the form

$$\begin{aligned}
\langle a \bar{b} \rangle &= 0, \\
\langle a b c c+1 \rangle &= 0, \\
\langle a a+1 \bar{b} \cap \bar{c} \rangle &= 0, \\
\langle a(a-1 a+1)(b b+1)(c c+1) \rangle &= 0,
\end{aligned}
\tag{3.30}$$

for arbitrary indices a, b, c . Again let us note that when we say there is a branch point at $x = 0$, we mean a branch cut between $x = 0$ and $x = \infty$. Indeed, this result is in precise accord with the known symbol alphabet of two-loop MHV amplitudes in SYM theory [34].

4 Discussion

In this paper we have improved greatly on the analysis of [17] by asking the amplituhedron directly to tell us which branch points of an amplitude are physical. This analysis requires no detailed knowledge about how to write formulas for integrands by constructing the canonical “volume” form on the amplituhedron. We only used the amplituhedron’s grossest feature, which is that it is designed to guarantee that integrands have no poles outside the space of positive loop configurations. We have shown in several examples how to use this principle to completely classify the sets of cut conditions on which integrands can possibly have support. Let us emphasize that our proposal is a completely well-defined geometric algorithm:

- Input: a list of the maximal codimension boundaries of the amplituhedron; for MHV amplitudes these are known from [5].
- Step 1: For a given maximal codimension boundary, identify the list of all cut conditions satisfied on this boundary. For example, at the two-loop boundary shown in figure 3a, these would be the nine cut conditions satisfied by the Landau diagram in figure 3b, shown in eqs. (3.7)–(3.9). Consider all lower codimension boundaries that can be obtained by relaxing various subsets of these cut conditions, and eliminate those which do not overlap the closure of the amplituhedron, i.e. those which do not correspond to mutually non-negative configurations of lines $\mathcal{L}^{(\ell)}$.
- Step 2: For each valid set of cut conditions obtained in this manner, solve the corresponding Landau equations (1.9) and (1.10) to determine the location of the corresponding branch point of the amplitude.

- Output: a list of the loci in external kinematic space where the given amplitude has branch points.

As we have mentioned a few times in the text, this algorithm is motivated by intuition from the Cutkosky rules, according to which an amplitude’s discontinuity is computed by replacing some set of propagators with delta-functions. This localizes the integral onto the intersection of the physical contour and the locus where the cut conditions are satisfied. Now is the time to confess that this intuitive motivation is not a proof of our algorithm, most notably because the positive kinematic domain lives in unphysical $(2, 2)$ signature and there is no understanding of how to make sense of the physical $i\epsilon$ contour in momentum twistor space (see however [38] for work in this direction). Nevertheless, the prescription works and it warrants serious further study, in part because it would be very useful to classify the possible branch points of more general amplitudes in SYM theory.

For amplitudes belonging to the class of generalized polylogarithm functions (which is believed to contain at least all MHV, NMHV and NNMHV amplitudes in SYM theory) the path from knowledge of branch points to amplitudes is fairly well-trodden. Such functions can be represented as iterated integrals [39] and analyzed using the technology of symbols and coproducts [40, 41]. It was emphasized in [16] that the analytic structure of an amplitude is directly imprinted on its symbol alphabet. In particular, the locus in external kinematic space where the letters of an amplitude’s symbols vanish (or diverge) must exactly correspond to the locus where solutions of the Landau equations exist. The above algorithm therefore provides direct information about the zero locus of an amplitude’s symbol alphabet. For example, the symbol alphabet of one-loop MHV amplitudes must vanish on the locus (3.6), and that of two-loop amplitudes must vanish on the locus (3.30). Strictly speaking this analysis does not allow one to actually determine symbol letters away from their vanishing locus, but it is encouraging that in both eqs. (3.6) and (3.30) the amplituhedron analysis naturally provides the correct symbol letters on the nose.

In general we expect that only letters of the type $\langle a a+1 b b+1 \rangle$ may appear in the first entry of the symbol of any amplitude [42]. At one loop, new letters of the type $\langle a \bar{b} \rangle$ begin to appear in the second entry. At two loops, additional new letters of the type $\langle a (a-1 a+1)(b b+1)(c c+1) \rangle$ also begin to appear in the second entry, and new letters of the type $\langle a b c c+1 \rangle$ and $\langle a a+1 \bar{b} \cap \bar{c} \rangle$ begin to appear in the third. As discussed at the end of section 3, the final entries of MHV amplitudes are always $\langle a \bar{b} \rangle$ [34]. In our paper we have given almost no thought to the question of where in the symbol a given type of letter may begin to appear. However, it seems clear that our geometric algorithm can be taken much further to expose this stratification of branch points, since the relationship

between boundaries of the amplituhedron and Landau singularities is the same as the relationship between discontinuities and their branch points. For example it is clear that at any loop order, the lowest codimension boundaries of the amplituhedron that give rise to branch cuts are configurations where one of the lines \mathcal{L} intersects two lines $(i\ i+1)$ and $(j\ j+1)$, with all other lines lying in generic mutually positive position. These configurations give rise to the expected first symbol entries $\langle i\ i+1\ j\ j+1 \rangle$. By systematically following the degeneration of configurations of lines onto boundaries of higher and higher codimension we expect there should be a way to derive the symbol alphabet of an amplitude entry by entry.

In many examples, mere knowledge of an amplitude’s symbol alphabet, together with some other physical principles, has allowed explicit formulas for the amplitude to be constructed via a bootstrap approach. This approach has been particularly powerful for 6- [43–48], and 7-point [49] amplitudes, in which case the symbol alphabet is believed to be given, to all loop order, by the set of cluster coordinates on the kinematic configuration space [50]. It would be very interesting to use the algorithm outlined above to prove this conjecture, or to glean information about symbol alphabets for more general amplitudes, both MHV and non-MHV. One simple observation we can make in parting is to note that although maximum codimension boundaries of the L -loop MHV amplitude involve as many as $2L$ distinct points, the singularities that arise from genuinely L -loop configurations (rather than products of lower loop order) involve at most $L + 1$ points. Therefore we predict that the size of the symbol alphabet of L -loop MHV amplitudes should grow with n no faster than $\mathcal{O}(n^{L+1})$.

It would be very interesting to extend our results to non-MHV amplitudes. For the N^K amplitude, singularities should still be found only on the boundary of the N^K MHV amplituhedron, so the presented approach should still be applicable, albeit more complicated. An important difference would be the existence of poles, in addition to branch points, due to the presence of rational prefactors. We are not certain our approach would naturally distinguish these two types of singularities. However, the singularities of rational prefactors can be found using other means, for example by considering the boundaries of the tree-level amplituhedron.

Acknowledgments

We have benefitted from very stimulating discussions with N. Arkani-Hamed and are grateful to J. J. Stankowicz for collaboration on closely related questions and for detailed comments on the draft. MS and AV are grateful to NORDITA and to the CERN theory group for hospitality and support during the course of this work. This work was supported by the US Department of Energy under contract DE-SC0010010 Task

A (MS, AV) and Early Career Award DE-FG02-11ER41742 (AV), as well as by Simons Investigator Award #376208 (AV).

A Elimination of Bubbles and Triangles

Here we collect a few comments on the elimination of bubble and triangle sub-diagrams in the Landau analysis. These tricks, together with the results of [17], can be used to easily obtain all of the Landau singularities reported in section 3.3.

A.1 Bubble sub-diagrams

The Landau equation for a bubble with propagators ℓ and $\ell + p$, which may be a sub-diagram of a larger diagram, are

$$\ell^2 = (\ell + p)^2 = 0, \quad (\text{A.1})$$

$$\alpha_1 \ell^\mu + \alpha_2 (\ell + p)^\mu = 0, \quad (\text{A.2})$$

where α_1 and α_2 are the Feynman parameters associated to the two propagators. The loop equation has solution

$$\ell^\mu = -\frac{\alpha_2}{\alpha_1 + \alpha_2} p^\mu \quad (\text{A.3})$$

so that

$$\alpha_1 \ell^\mu = -\frac{\alpha_1 \alpha_2}{\alpha_1 + \alpha_2} p^\mu, \quad \alpha_2 (\ell + p)^\mu = \frac{\alpha_1 \alpha_2}{\alpha_1 + \alpha_2} p^\mu, \quad (\text{A.4})$$

while the on-shell conditions simply impose $p^2 = 0$. Therefore, we see that any Landau diagram containing this bubble sub-diagram is equivalent to the same diagram with the bubble replaced by a single on-shell line with momentum p^μ and modified Feynman parameter $\alpha' = \alpha_1 \alpha_2 / (\alpha_1 + \alpha_2)$. We do not need to keep track of the modified Feynman parameter; we simply move on to the rest of the diagram using the new Feynman parameter α' .

In conclusion, any bubble sub-diagram can be collapsed to a single edge, as far as the Landau analysis is concerned.

A.2 Triangle sub-diagrams

Similarly, we will now discuss the various branches associated to a triangle sub-diagram. The Landau equations for a triangle with edges carrying momenta $q_1 = \ell$, $q_2 = \ell + p_1 + p_2$ and $q_3 = \ell + p_2$, and with corresponding Feynman parameters α_1 , α_2 and α_3 , are

$$\ell^2 = (\ell + p_2)^2 = (\ell + p_1 + p_2)^2 = 0, \quad (\text{A.5})$$

$$\alpha_1 \ell^\mu + \alpha_2 (\ell + p_1 + p_2)^\mu + \alpha_3 (\ell + p_2)^\mu = 0. \quad (\text{A.6})$$

The solution to the loop equation is

$$\ell^\mu = -\frac{(\alpha_2 + \alpha_3)p_2^\mu + \alpha_2 p_1^\mu}{\alpha_1 + \alpha_2 + \alpha_3} \quad (\text{A.7})$$

while eqs. (A.5) impose the two conditions

$$0 = p_1^2 p_2^2 p_3^2, \quad (\text{A.8})$$

$$(\alpha_1 : \alpha_2 : \alpha_3) = (p_1^2(-p_1^2 + p_2^2 + p_3^2) : p_2^2(p_1^2 - p_2^2 + p_3^2) : p_3^2(p_1^2 + p_2^2 - p_3^2)) \quad (\text{A.9})$$

where $p_3 = -p_1 - p_2$. Suppose we follow the branch $p_1^2 = 0$. In this case α_1 is forced to vanish, effectively reducing the triangle to a bubble with edges

$$\alpha_2 q_2^\mu = \frac{\alpha_3 p_2^2}{p_2^2 - p_3^2} p_1^\mu, \quad \alpha_3 q_3^\mu = -\frac{\alpha_3 p_2^2}{p_2^2 - p_3^2} p_1^\mu. \quad (\text{A.10})$$

This is equivalent (by appendix A.1) to a single on-shell line carrying momentum p_1^μ . A similar conclusion clearly holds for the branches $p_2^2 = 0$ or $p_3^2 = 0$. If any two of p_1^2 , p_2^2 or p_3^2 simultaneously vanish, then the two corresponding Feynman parameters must vanish. Finally, if all three p_i^2 vanish, then the Landau equations are identically satisfied for any values of the three α_i . In conclusion, triangle sub-diagrams of a general Landau diagram can be analyzed by considering separately each of the seven branches outlined here.

References

- [1] L. Brink, J. H. Schwarz and J. Scherk, ‘‘Supersymmetric Yang-Mills Theories,’’ Nucl. Phys. B **121**, 77 (1977). doi:10.1016/0550-3213(77)90328-5
- [2] N. Arkani-Hamed, J. L. Bourjaily, F. Cachazo, S. Caron-Huot and J. Trnka, ‘‘The All-Loop Integrand For Scattering Amplitudes in Planar $\mathcal{N} = 4$ SYM,’’ JHEP **1101**, 041 (2011) doi:10.1007/JHEP01(2011)041 [arXiv:1008.2958 [hep-th]].
- [3] N. Arkani-Hamed, J. L. Bourjaily, F. Cachazo, A. B. Goncharov, A. Postnikov and J. Trnka, ‘‘Scattering Amplitudes and the Positive Grassmannian,’’ arXiv:1212.5605 [hep-th].
- [4] N. Arkani-Hamed and J. Trnka, ‘‘The Amplituhedron,’’ JHEP **1410**, 030 (2014) doi:10.1007/JHEP10(2014)030 [arXiv:1312.2007 [hep-th]].
- [5] N. Arkani-Hamed and J. Trnka, ‘‘Into the Amplituhedron,’’ JHEP **1412**, 182 (2014) doi:10.1007/JHEP12(2014)182 [arXiv:1312.7878 [hep-th]].
- [6] Y. Bai and S. He, ‘‘The Amplituhedron from Momentum Twistor Diagrams,’’ JHEP **1502**, 065 (2015) doi:10.1007/JHEP02(2015)065 [arXiv:1408.2459 [hep-th]].

- [7] S. Franco, D. Galloni, A. Mariotti and J. Trnka, “Anatomy of the Amplituhedron,” *JHEP* **1503**, 128 (2015) doi:10.1007/JHEP03(2015)128 [arXiv:1408.3410 [hep-th]].
- [8] T. Lam, “Amplituhedron cells and Stanley symmetric functions,” *Commun. Math. Phys.* **343**, no. 3, 1025 (2016) doi:10.1007/s00220-016-2602-2 [arXiv:1408.5531 [math.AG]].
- [9] N. Arkani-Hamed, A. Hodges and J. Trnka, “Positive Amplitudes In The Amplituhedron,” *JHEP* **1508**, 030 (2015) doi:10.1007/JHEP08(2015)030 [arXiv:1412.8478 [hep-th]].
- [10] Y. Bai, S. He and T. Lam, “The Amplituhedron and the One-loop Grassmannian Measure,” *JHEP* **1601**, 112 (2016) doi:10.1007/JHEP01(2016)112 [arXiv:1510.03553 [hep-th]].
- [11] L. Ferro, T. Lukowski, A. Orta and M. Parisi, “Towards the Amplituhedron Volume,” *JHEP* **1603**, 014 (2016) doi:10.1007/JHEP03(2016)014 [arXiv:1512.04954 [hep-th]].
- [12] Z. Bern, E. Herrmann, S. Litsey, J. Stankowicz and J. Trnka, “Evidence for a Nonplanar Amplituhedron,” *JHEP* **1606**, 098 (2016) doi:10.1007/JHEP06(2016)098 [arXiv:1512.08591 [hep-th]].
- [13] D. Galloni, “Positivity Sectors and the Amplituhedron,” arXiv:1601.02639 [hep-th].
- [14] L. J. Dixon, J. M. Drummond, C. Duhr, M. von Hippel and J. Pennington, “Bootstrapping six-gluon scattering in planar $\mathcal{N} = 4$ super-Yang-Mills theory,” *PoS LL* **2014**, 077 (2014) [arXiv:1407.4724 [hep-th]].
- [15] J. Golden and M. Spradlin, “A Cluster Bootstrap for Two-Loop MHV Amplitudes,” *JHEP* **1502**, 002 (2015) doi:10.1007/JHEP02(2015)002 [arXiv:1411.3289 [hep-th]].
- [16] J. Maldacena, D. Simmons-Duffin and A. Zhiboedov, “Looking for a bulk point,” *JHEP* **1701**, 013 (2017) doi:10.1007/JHEP01(2017)013 [arXiv:1509.03612 [hep-th]].
- [17] T. Dennen, M. Spradlin and A. Volovich, “Landau Singularities and Symbology: One- and Two-loop MHV Amplitudes in SYM Theory,” *JHEP* **1603**, 069 (2016) doi:10.1007/JHEP03(2016)069 [arXiv:1512.07909 [hep-th]].
- [18] S. Mandelstam, “Determination of the pion–nucleon scattering amplitude from dispersion relations and unitarity. General theory,” *Phys. Rev.* **112**, 1344 (1958). doi:10.1103/PhysRev.112.1344
- [19] S. Mandelstam, “Analytic properties of transition amplitudes in perturbation theory,” *Phys. Rev.* **115**, 1741 (1959). doi:10.1103/PhysRev.115.1741
- [20] L. D. Landau, “On analytic properties of vertex parts in quantum field theory,” *Nucl. Phys.* **13**, 181 (1959). doi:10.1016/0029-5582(59)90154-3

- [21] R. E. Cutkosky, “Singularities and discontinuities of Feynman amplitudes,” *J. Math. Phys.* **1**, 429 (1960). doi:10.1063/1.1703676
- [22] Z. Bern, L. J. Dixon, D. C. Dunbar and D. A. Kosower, “Fusing gauge theory tree amplitudes into loop amplitudes,” *Nucl. Phys. B* **435**, 59 (1995) doi:10.1016/0550-3213(94)00488-Z [hep-ph/9409265].
- [23] Z. Bern, L. J. Dixon and D. A. Kosower, “Progress in one loop QCD computations,” *Ann. Rev. Nucl. Part. Sci.* **46**, 109 (1996) doi:10.1146/annurev.nucl.46.1.109 [hep-ph/9602280].
- [24] S. Abreu, R. Britto, C. Duhr and E. Gardi, “From multiple unitarity cuts to the coproduct of Feynman integrals,” *JHEP* **1410**, 125 (2014) doi:10.1007/JHEP10(2014)125 [arXiv:1401.3546 [hep-th]].
- [25] S. Abreu, R. Britto and H. Grönqvist, “Cuts and coproducts of massive triangle diagrams,” *JHEP* **1507**, 111 (2015) doi:10.1007/JHEP07(2015)111 [arXiv:1504.00206 [hep-th]].
- [26] N. Arkani-Hamed, J. L. Bourjaily, F. Cachazo and J. Trnka, “Local Integrals for Planar Scattering Amplitudes,” *JHEP* **1206**, 125 (2012) doi:10.1007/JHEP06(2012)125 [arXiv:1012.6032 [hep-th]].
- [27] A. Hodges, “Eliminating spurious poles from gauge-theoretic amplitudes,” *JHEP* **1305**, 135 (2013) doi:10.1007/JHEP05(2013)135 [arXiv:0905.1473 [hep-th]].
- [28] R. J. Eden, P. V. Landshoff, D. I. Olive and J. C. Polkinghorne, “The Analytic S-Matrix,” Cambridge University Press, 1966.
- [29] S. Coleman and R. E. Norton, “Singularities in the physical region,” *Nuovo Cim.* **38**, 438 (1965). doi:10.1007/BF02750472
- [30] S. J. Parke and T. R. Taylor, “An Amplitude for n Gluon Scattering,” *Phys. Rev. Lett.* **56**, 2459 (1986). doi:10.1103/PhysRevLett.56.2459
- [31] D. B. Fairlie, P. V. Landshoff, J. Nuttall and J. C. Polkinghorne, “Singularities of the Second Type,” *J. Math. Phys.* **3**, 594 (1962). doi:10.1063/1.1724262
- [32] D. B. Fairlie, P. V. Landshoff, J. Nuttall and J. C. Polkinghorne, “Physical sheet properties of second type singularities,” *Phys. Lett.* **3**, 55 (1962). doi:10.1016/0031-9163(62)90200-7
- [33] Z. Bern, L. J. Dixon, D. C. Dunbar and D. A. Kosower, “One loop n point gauge theory amplitudes, unitarity and collinear limits,” *Nucl. Phys. B* **425**, 217 (1994) doi:10.1016/0550-3213(94)90179-1 [hep-ph/9403226].
- [34] S. Caron-Huot, “Superconformal symmetry and two-loop amplitudes in planar $\mathcal{N} = 4$ super Yang-Mills,” *JHEP* **1112**, 066 (2011) doi:10.1007/JHEP12(2011)066 [arXiv:1105.5606 [hep-th]].

- [35] J. L. Bourjaily and J. Trnka, “Local Integrand Representations of All Two-Loop Amplitudes in Planar SYM,” *JHEP* **1508**, 119 (2015) doi:10.1007/JHEP08(2015)119 [arXiv:1505.05886 [hep-th]].
- [36] T. Dennen, unpublished notes.
- [37] Z. Bern, L. J. Dixon and V. A. Smirnov, “Iteration of planar amplitudes in maximally supersymmetric Yang-Mills theory at three loops and beyond,” *Phys. Rev. D* **72**, 085001 (2005) doi:10.1103/PhysRevD.72.085001 [hep-th/0505205].
- [38] A. E. Lipstein and L. Mason, “From d logs to dilogs; the super Yang-Mills MHV amplitude revisited,” *JHEP* **1401**, 169 (2014) doi:10.1007/JHEP01(2014)169 [arXiv:1307.1443 [hep-th]].
- [39] K. T. Chen, “Iterated path integrals”, *Bull. Amer. Math. Soc.* **83**, (1977), 831–879. doi:10.1090/S0002-9904-1977-14320-6
- [40] A. B. Goncharov, “A simple construction of Grassmannian polylogarithms,” [arXiv:0908.2238v2 [math.AG]].
- [41] A. B. Goncharov, M. Spradlin, C. Vergu and A. Volovich, “Classical Polylogarithms for Amplitudes and Wilson Loops,” *Phys. Rev. Lett.* **105**, 151605 (2010) doi:10.1103/PhysRevLett.105.151605 [arXiv:1006.5703 [hep-th]].
- [42] D. Gaiotto, J. Maldacena, A. Sever and P. Vieira, “Pulling the straps of polygons,” *JHEP* **1112**, 011 (2011) doi:10.1007/JHEP12(2011)011 [arXiv:1102.0062 [hep-th]].
- [43] L. J. Dixon, J. M. Drummond and J. M. Henn, “Bootstrapping the three-loop hexagon,” *JHEP* **1111**, 023 (2011) doi:10.1007/JHEP11(2011)023 [arXiv:1108.4461 [hep-th]].
- [44] L. J. Dixon, J. M. Drummond, M. von Hippel and J. Pennington, “Hexagon functions and the three-loop remainder function,” *JHEP* **1312**, 049 (2013) doi:10.1007/JHEP12(2013)049 [arXiv:1308.2276 [hep-th]].
- [45] L. J. Dixon, J. M. Drummond, C. Duhr and J. Pennington, “The four-loop remainder function and multi-Regge behavior at NNLLA in planar $\mathcal{N} = 4$ super-Yang-Mills theory,” *JHEP* **1406**, 116 (2014) doi:10.1007/JHEP06(2014)116 [arXiv:1402.3300 [hep-th]].
- [46] L. J. Dixon and M. von Hippel, “Bootstrapping an NMHV amplitude through three loops,” *JHEP* **1410**, 065 (2014) doi:10.1007/JHEP10(2014)065 [arXiv:1408.1505 [hep-th]].
- [47] L. J. Dixon, M. von Hippel and A. J. McLeod, “The four-loop six-gluon NMHV ratio function,” *JHEP* **1601**, 053 (2016) doi:10.1007/JHEP01(2016)053 [arXiv:1509.08127 [hep-th]].

- [48] S. Caron-Huot, L. J. Dixon, A. McLeod and M. von Hippel, “Bootstrapping a Five-Loop Amplitude Using Steinmann Relations,” *Phys. Rev. Lett.* **117**, no. 24, 241601 (2016) doi:10.1103/PhysRevLett.117.241601 [arXiv:1609.00669 [hep-th]].
- [49] J. M. Drummond, G. Papathanasiou and M. Spradlin, “A Symbol of Uniqueness: The Cluster Bootstrap for the 3-Loop MHV Heptagon,” *JHEP* **1503**, 072 (2015) doi:10.1007/JHEP03(2015)072 [arXiv:1412.3763 [hep-th]].
- [50] J. Golden, A. B. Goncharov, M. Spradlin, C. Vergu and A. Volovich, “Motivic Amplitudes and Cluster Coordinates,” *JHEP* **1401**, 091 (2014) doi:10.1007/JHEP01(2014)091 [arXiv:1305.1617 [hep-th]].